Thermochimica Acta 511 (2010) 17–26

Contents lists available at ScienceDirect

Thermochimica Acta

journal homepage: www.elsevier.com/locate/tca

Synthesis, characterization and thermal degradation of 1-D coordination polymers of the type Cu_xZn_{1-x}(dadb)·yH_2O (dadb = 2,5-diamino-3,6-dichloro-1,4-benzoquinone; and x = 1.0, 0.5, 0.0625 and 0)

R.L. Prasad*, Anita Kushwaha, Deepshikha Singh

Department of Chemistry, Faculty of Science, BHU, Varanasi 221005, India

ARTICLE INFO

Article history:
Received 16 April 2010
Received in revised form 6 July 2010
Accepted 20 July 2010
Available online 27 July 2010

Keywords:
1-D coordination polymer
Metal complexes of 2,5-diamino-3,6-dichloro-1,4-benzoquinone
Heterobimetallic complexes
Thermal analysis of 1-D polymers

ABSTRACT

New complexes of the type [{$M_xM'_{1-x}$(dadb)}$_n$·yH_2O] {where dadbH_2 = 2,5-diamino-3,6-dichloro-1,4-benzoquinone (1); M = Cu(II); M′ = Zn(II); x = 1 (2), 0.5 (4), 0.0625 (5), 0 (3); y = 0–2 and n = degree of polymerization} were synthesized and characterized. Distinct identities of heterobimetallic complexes are revealed from nature and position of their PXRD lines. Complexes under present study are hygroscopic in the temperature range RT–60 °C. The TGA, DTA and DSC thermograms suggest that complexes first lose water molecules followed by loss of HCl molecules under 2nd step of thermal degradation which is catalyzed by Cu(II) ions, whereas elimination of CO under 3rd step is catalyzed by air. Residue from 2 and 3 corresponds to 1/2 mole of metallic copper and zinc, respectively, under nitrogen atmosphere, whereas, one mole of CuO and half mole of ZnO, respectively under air. Thermal degradation pattern of the ligand moiety around Cu(II) have been observed to be different than that around Zn(II) ion.

1. Introduction

The dadb molecule is reported to possess two parallel conjugated strands (Fig. 1a) across the molecule [1–3]. Supramolecular structure (Fig. 1b) of the 2,5-diamino-3,6-dichloro-1,4-benzoquinone (dadb) molecule [4] shows one dimensional stacking through π–π interaction between ring carbon atoms of adjacent molecules and exhibits metallic conductivity. Due to presence of donor atoms at each end of conjugated strands of the dadb molecule, it is expected to form 1-D coordination polymer like that of CA (chloranilic acid) [5] (Fig. 1c). Two metal ions coordinated simultaneously to same conjugated dadb ligand are expected to be in electronic communication with each other like Creutz-Taube ion [6,7] (Fig. 1d). The extent of electronic communication depends upon nature of metal ion and intermittent ligand [7]. During electronic communication between two metal ion, electron (charge densities) will pass through intermittent coordinated ligand, i.e. electron of metal ion will be delocalized on ligand. Consequently, charge density on various atoms of the coordinated ligand may vary upon variation of adjacent metal ion coordinated to ligand in 1-D chain. Thus, coordination polymer of transition metal ions with π-conjugated ligand dadb is expected to exhibit their application as good conducting material as metallic/semiconducting materials [8]. Therefore, study of thermal stability of such useful materials is foremost important and is undertaken. Further, thin film deposition (MOCVD) of metal and metal oxides have been achieved by pyrolytic cleavage of metal complexes for their application in electronic industries [9]. Metal/metal oxides formed under different environment exhibit different characteristics, therefore, thermal studies of the new title metal complexes were under taken to predict the pyrolytic product which may be useful in future as gas sensors [10], optical switch [11], magnetic storage media [12], lithium batteries [13], solar cells [14] owing to its photoconductive and photochemical properties and catalyst [15].

Electronic environment on the ligand atoms changes by varying the adjacent coordinated metal ion in 1-D coordination polymer, therefore, it may be expected that the thermal degradation of the ligand moiety of the complexes should be influenced by changing the coordinated metal ion. This may change morphology, texture and composition of useful pyrolytic product hence its properties [16,17]. In view of above, present investigation was under taken to study the thermal stability, degradation pattern, final pyrolytic product and observe variation of degradation pattern and final residue of heterobimetallic complexes w.r.t. their monometallic complexes. Further, the reports on metal complexes of dadb are lacking except one study on thermovolumetric [18] measurement of cobalt(II), iron(II) and manganese(II) complexes of dadb under

* Corresponding author. Tel.: +91 542 6702487; fax: +91 542 2368127.
E-mail address: rlpjc@yahoo.co.in (R.L. Prasad).

0040-6031/$ – see front matter © 2010 Elsevier B.V. All rights reserved.
doi:10.1016/j.tca.2010.07.019

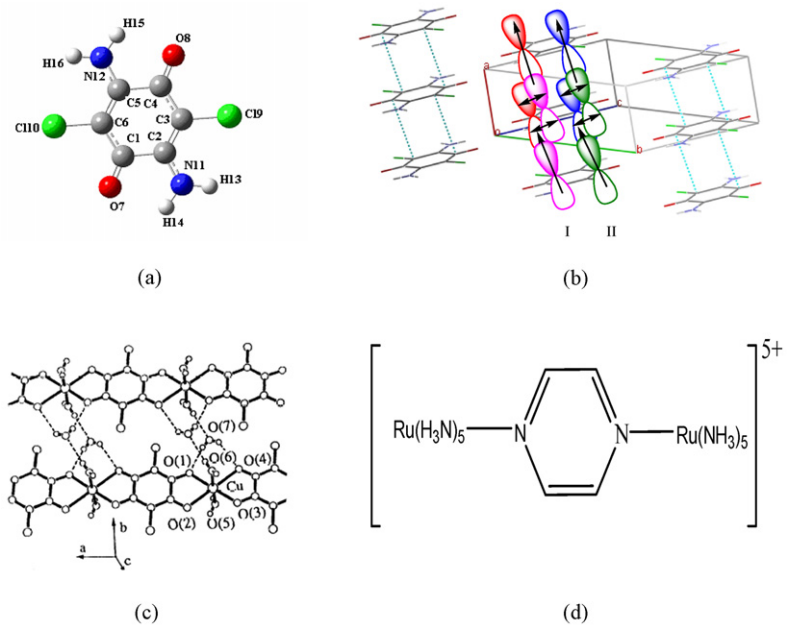

Fig. 1. (a) Optimized molecular structure of 1. (b) 1-D stacking via π–π interactions. (c) Structure of $[Cu(CA)]_n$. (d) Creutz-Taube ion.

nitrogen atmosphere upto 300 °C. In present communication synthesis, characterization and thermal degradation pattern of 1-D coordination polymers of the type Cu_xZn_{1-x}(dadb) (x = 1.0, 0.5, 0.0625 and 0) is being reported.

2. Experimental

2.1. Physico-chemical measurements

The elemental analysis (Carbon, hydrogen and nitrogen) was performed on a Elemental Analyzer model Carlo Erba 1108. Magnetic susceptibility of the powdered samples was measured at room temperature on a Cahn-Faraday electro balance using $[CoHg(NCS)_4]$ as calibrant. The melting points of the complexes were determined in open capillaries using Gallenkamp apparatus and are uncorrected. Electronic absorption spectra were recorded on a UV-1700 PHARMA SPEC UV–visible spectrophotometer in solid state as Nujol mulls. IR spectra on KBr disc were recorded on a VARIAN 3100 FT-IR spectrophotometer in the region 4000–400 cm^{-1}. The X-ray powder diffraction patterns were recorded on X-ray diffraction SEIFERT RICH. SEIFERT and Co. Gmbh and Co. KG D-2070 Ahrensburg using Cu Kα-radiation and Rigaku D. Max-B Powder X-ray diffractometer with Cu Kα-radiation. The thermogravimetric analysis curves (TGA, DTG and DTA) were recorded on Perkin Elmer, Diamond TG/DTA and NETZSCH STA 409 C/CD. DSC thermograms were recorded on Mettler Toledo TC 15 TA differential scanning calorimeter at rate of 5 °C/min under nitrogen atmosphere using Spec. pure grade indium as standard by taking samples in closed lid aluminium pan. The variable temperature electrical conductivity of the metal complexes was measured using conventional two-probe technique on a Keithley 236 source measure unit.

2.2. Synthesis of metal complexes

All the chemicals used under present investigations were of analytical reagent grade. Solvent were purified and dried prior to the use by standard methods [19]. The ligand 2,5-diamino-3,6-dichloro-1,4-benzoquinone (1) was prepared following literature procedure [18,20].

2.2.1. Metal complexes of the type $[M(dadb)]_n \cdot xH_2O$ [$M = Cu^{2+}$ (2), Zn^{2+} (3)]

To a 0.414 g dadb (2 mmol) and 0.224 g KOH (4 mmol) dissolved in 40 ml 50% ethanolic solution, a solution of metal salt (2 mmol) dissolved in 15 ml distilled water was added slowly drop wise with constant stirring in 30 min and continued stirring for further 5 h. Reaction mixture was heated for 30 min over water bath and allowed to stand at room temperature for 2 h. The precipitated complexes were filtered washed with distilled water thrice. The precipitated complexes were purified by stirring for one hr in a solvent mixture consist of 25% ethanol, 25% acetone, 5% DMF and 45% distilled water and filtered, washed with distilled water thrice followed by ethanol and dried under vacuo over anhydrous $CaCl_2$.

2.2.2. Synthesis of heterobimetallic complexes

2.2.2.1. $Cu_{0.5}Zn_{0.5}(dadb)\cdot xH_2O$ (4). The heterobimetallic complex $Cu_{0.5}Zn_{0.5}$(dadb)·xH_2O was synthesized by adding a 10 ml homogeneous aqueous solution of $ZnSO_4 \cdot 7H_2O$ (0.287 g, 1 mmol) and $CuSO_4 \cdot 5H_2O$ (0.250 g, 1 mmol) into a pink colored 50% ethanolic solution (40 ml) of dadb (0.414 g, 2 mmol) and KOH (0.224 g, 4 mmol) drop wise with constant stirring over a period of 1/2 h. The reaction mixture turned to intense dark color solution. The reaction mixture was further stirred for 5 h followed by digestion over water bath for 30 min and cooled to room temperature. Subsequently same procedures were followed as in Section 2.2.1.

2.2.2.2. $Cu_{0.0625}Zn_{0.9375}(dadb)\cdot xH_2O$ (5). The heterobimetallic complex $Cu_{0.0625}Zn_{0.9375}$dadb was synthesized by adding an aqueous solution of $ZnSO_4 \cdot 7H_2O$ (0.539 g, 1.88 mmol) + $CuSO_4 \cdot 5H_2O$ (0.031 g, 0.12 mmol) into a pink colored 50% ethanolic solution (40 ml) of dadb (0.414 g, 2 mmol) and KOH (0.224 g, 4 mmol) drop wise with constant stirring over a period of 1/2 h. Rest procedure was same as described in Section 2.2.1.

3. Results and discussion

Analytical data agree with composition of the complexes given in Table 1. The solid complexes are stable in presence of air but weakly hygroscopic. Complexes dried over $CaCl_2$ under vacuo gain some weight on exposure to air and extent of weight gain depends

Table 1
Analytical data and physical properties of the complexes.

Compound Compound no.	Color	Yield (%)	C	H	N	M.P.[a] (°C)
Cudadb·2H_2O 2	Blackish green	65	24.24 (23.65)	1.97 (1.97)	8.63 (9.19)	>280
$Cu_{0.5}Zn_{0.5}$dadb·2H_2O 4	Gray	84	22.95 (23.57)	1.56 (1.96)	8.74 (9.17)	275–278[a]
$Cu_{0.0625}Zn_{0.9375}$dadb·2H_2O 5	Gray	66	23.93 (23.51)	1.73 (1.96)	8.70 (9.14)	277–280[a]
Zndadb·H_2O 3	Dark pink	72	25.54 (24.97)	1.78 (1.38)	9.24 (9.71)	>300

[a] Decomposition temperature.

Table 2
X-ray powder diffraction data of the complexes.

Compound	Position of intense and distinct peaks (2θ)				
	I	II	III	IV	V
1	12.75			25.11, 26.59	27.46, 28.93, 29.80, 31.69, 45.53, 56.39, 66.38, 73.32
2	14.16	18.96	22.48	25.44	27.8
4	13.52	19.52	22.96	–	27.56
5	13.48	19.64	22.32	24.85sh	27.16
3	12.0, 13.84	18.26	21.96	23.84	–

sh = shoulder.

upon relative humidity present in air. They decompose in the temperature range 275–300 °C. All the metal complexes are insoluble in common organic solvents such as ethanol, methanol, acetone, chloroform, dichloromethane, ether and benzene as well as highly polar solvent like DMF and DMSO.

3.1. IR spectra

The spectrum of the ligand dadb in KBr exhibits two band at 3308 and 3376 cm^{-1} due to $\nu_s(NH_2)_{opc}$ and $\nu_{as}(NH_2)_{opc}$ modes of the NH_2 groups [1]. The other characteristic ligand bands at 1667, 1616 and 1580 cm^{-1} are assigned to ν(C=O), ν(C=C ring) and βNH_2 modes of vibrations, respectively [1]. The metal complexes of the dadb exhibit ν(OH) stretching frequencies as a broad band in the range 3421–3470 cm^{-1} which is absent in the parent ligand. Presence of ν(OH) stretching frequencies in the metal complexes indicates the presence of water molecules in the complexes. Metal complexes exhibit only one band corresponding to ν_{as}(N–H) stretching vibration. This indicates that one of the hydrogen atoms of NH_2 groups is absent due to deprotonation. The decrease of the wave number value for the NH stretching vibration of the metal complexes as compared to that of the ligand dadb suggests that nitrogen atom of the NH_2 group is involved in coordination. Asymmetric (C=O) stretching vibration mode of the metal complexes are observed in the range 1600–1647 cm^{-1} as medium intensity band either as shoulder or as distinct peak, whereas, this peak is observed as distinct peak at 1667 cm^{-1} in the ligand dadb. Thus lowering of ν_{as}(C=O) frequency in the metal complexes indicate coordinated nature of carbonyl group [21,22]. The ν(C=C) and βNH_2 mode of vibrations of the ligand merge and yield a single broad band into their metal complexes except in case of the Cudadb where ν(C=C) is observed as distinct shoulder at 1542 and βNH_2 mode at 1494 cm^{-1}. Shifting of these bands to lower wave number in their metal complexes as compare to that found in the free dadb ligand support coordinated nature of the dadb ligand.

3.2. Powder XRD spectra

The powder XRD spectra of complexes recorded between 2θ values 10° and 80° exhibit many lines suggesting the crystalline [5,23,24] nature of these complexes. Distinguished peaks present in the PXRD spectrum of each of the complexes 2–5 are divided into five major ranges (I–V) (Table 2 and Fig. 2). There are two peaks in the diffractogram of 3 in between 2θ values 12° and 14° whereas other complexes 2, 4 and 5 exhibit only one peak in this region which is most intense (I). For the heterobimetallic complexes 4 and 5, position of the most intense peak falls between corresponding peak positions for the monometallic complexes 2 and 3. Second intense peak (II) of heterobimetallic complexes 4 and 5 are observed as broad and at higher 2θ values than those of corresponding peak in the monometallic complexes 2 and 3. Third intense peak (III) of the complex 4 is also obtained at higher 2θ value than those of complexes 2 and 3. However, this peak of complex 5 is observed at slightly lower 2θ value than that of 2 but higher than that of 3. Position of fourth intense peak (IV) in 5 lies between those of 2 and 3 as shoulder whereas corresponding peak is absent in complex 4. Position of fifth peak in the heterobimetallic complexes 4 and 5 are very close to that of 2. The peak corresponding to fifth peak between 27° and 28° in the complex 3 is very weak and is not well

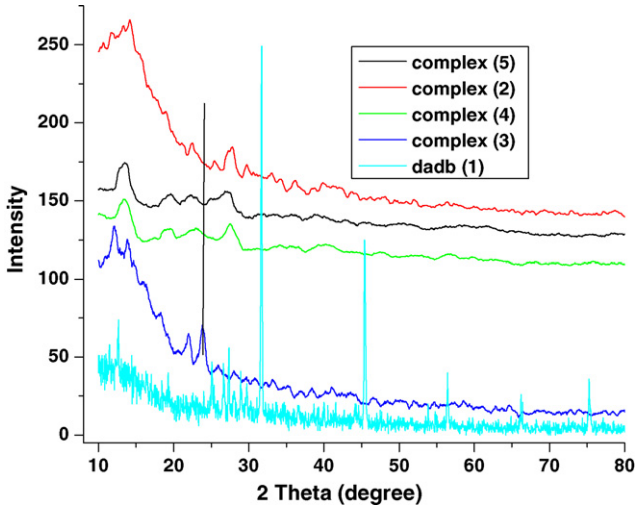

Fig. 2. Powder X-ray diffraction pattern of the complexes 2, 3,4 and 5.

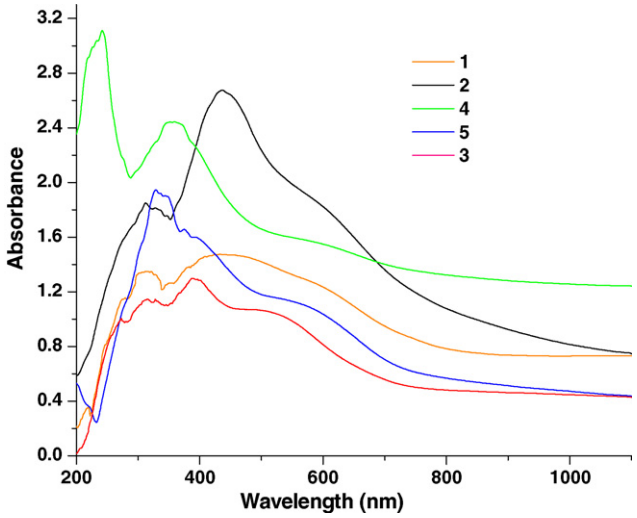

Fig. 3. UV–visible absorption spectra of the compounds 1–5.

marked. Thus, the nature and positions of X-ray diffraction peaks of 4 and 5 are entirely different from those observed for 2 and 3. These results indicate that the complexes 4 and 5 are new entities rather than mixtures of 2 and 3.

3.3. Magnetic moments and electronic spectra

Magnetic and solid state electronic spectra of the ligand 1 and metal complexes 2–5 are given in Fig. 3 and Table 3. The μ_{eff} value of complex 2 is slightly less than that expected from one unpaired electron probably due to antiferromagnetic interaction between neighbouring copper centres [5]. Other heterobimetallic complexes show magnetic moment corresponding to one unpaired electron [25,26]. Zinc metal complex 3 is diamagnetic. On the basis of nature and position of the peaks a square-planar geometry may be tentatively proposed of the complex 2 [26,27]. Due to similarity of peak positions of first and second peaks of 4 and 5 with those of 2 a square-planar structure around copper metal ion in heterobimetallic complexes may be proposed.

3.4. Thermal analysis

Thermal studies of the monometallic and heterobimetallic complexes of dadb in various mole ratios of metal ions have been carried out under nitrogen and air atmosphere. The thermogravimetric analyses (TGA, DTG and DTA) of complexes were recorded in the temperature range RT–1000 °C and are presented in Fig. 4a–f. DTG curves of all the complexes under nitrogen and air atmospheres are given S.I. Fig. 1a and b, respectively. Differential scanning calorimetry (DSC) curves for complexes 3 and 2 have been represented in Fig. 4g. The weight losses in various temperature ranges on thermal degradation of the complexes under nitrogen and air atmospheres are given in supplementary information (S.I.) Table 1(a)–(f) along with position of peaks in DTG and DTA thermograms. Plausible tentative thermal degradation pattern proposed for the metal complexes under nitrogen are presented in Scheme 1(A) and (B), and under air in Scheme 2(A) and (B).

Thomas Allmendinger [18] studied cobalt(II), iron(II) and manganese(II) complexes of dadb thermo-volumetrically by heating complexes up to 300 °C under nitrogen atmosphere and found that quantitative amount of HCl gas is lost from cobalt and manganese complexes but smaller amount of HCl is lost from iron complexes. It was concluded that part of the chloride is consumed in complexation with iron metal ions. Thus, it is obvious that there are two possibilities during thermal degradation of metal complexes of dadb: (i) all the liberated HCl molecules escape or (ii) one part of the liberated HCl molecules react with metal ions to form metal chlorides, liberate hydrogen and ligand residue while remaining part of HCl escapes. Based on possibility (i) the Schemes 1A and 2A have been proposed for thermal degradation of metal complexes under nitrogen and air atmospheres, respectively. Similarly Schemes 1B and 2B have been proposed for thermal degradation of metal complexes under nitrogen and air atmospheres on the basis of possibility (ii). The weight losses calculated for various steps of the thermal degradation of 2 under nitrogen atmosphere on the basis of Scheme 1A and B are presented in S.I. Table 1(a). Experimentally obtained weight losses from TGA curve with help of corresponding DTG curve are also included in the table along with calculated values (in parenthesis).

First stage of weight loss corresponds to the loss of water molecule under air as well as nitrogen atmosphere for all the complexes. Loss of water molecules take place in the temperature range RT–200 °C in most of the complexes and are associated with one or two peaks in its DTG curve and corresponding endothermic peaks in DTA thermogram of all the complexes. It is worth to be mentioned that the sample dried under vacuum gains some weight on exposure to air by absorbing the water molecules. Further, presence of exothermic peaks in the DTA curve for some of the complexes in the temperature range RT–60 °C indicates absorption of moisture by the samples on exposure to air. The amounts of water molecules absorbed vary upon the variation of relative humidity present in the air. Both the DTA and DSC curves for 3 (Fig. 4g) exhibit endothermic curve corresponding to water loss in temperature range RT–200 °C. In case of 2 the broad endothermic peak is present in its DTA curve, however, DSC curve recorded for the sample of 2 (Fig. 4g) dried under vacuo over $CaCl_2$ exhibits no peak in the temperature range 40–200 °C indicating the presence of non-coordinated nature of water molecules. Therefore, it may be concluded that water molecules present on/near to surface of sample are lost at lower temperature and as the complexes are polymeric therefore, crystalline water molecules trapped inside the polymeric matrix are lost at higher temperatures. The DTG and DTA peaks observed above 100 °C are probably due to delayed elimination of trapped crystalline water molecules.

In second step of thermal degradation two HCl molecules are expected to be lost under Scheme 1A, whereas under Scheme 1B it is assumed that one out of two moles of HCl molecules are liberated on heating the complex 2, i.e. one mole of HCl molecules react with copper ions to form half mole of $CuCl_2$ and hydrogen gas molecules and other half of the HCl molecules (one mole) escapes [18]. Due to above reaction, half of ligand fragments are expected to remain bonded with metal, whereas other half of the ligand moiety become free from metal. The free ligand fragment obtained is expected to lose 1/2 moles of $(CN)_2$ and H_2 molecules. The net weight loss under Scheme 1A and B are calculated to be 37.63% and 34.60%, respectively from 2 under nitrogen atmosphere. Calculated weight loss following Scheme 1B from 2 falls on the curvature of the DTG peak suggesting that Scheme 1B being followed for degradation of this complex is unlikely. However, the observed weight loss 37% from TGA curve coinciding with slowest rate of weight loss in the DTG

Table 3
Magnetic moment data and electronic absorption bands of the complexes.

Compound	Magnetic moment (BM)	λ_{max} (cm^{-1}) as nujol mull
1	–	16722, 22573, 32051, 36316, 37736, 46083
2	1.63	16502, 23148, 31847
4	2.03	16892,27933,40983, 46511
5	1.92	17544, 25316, 26455, 28818, 30488
3	Diamagnetic	19011, 25316, 32051, 36765

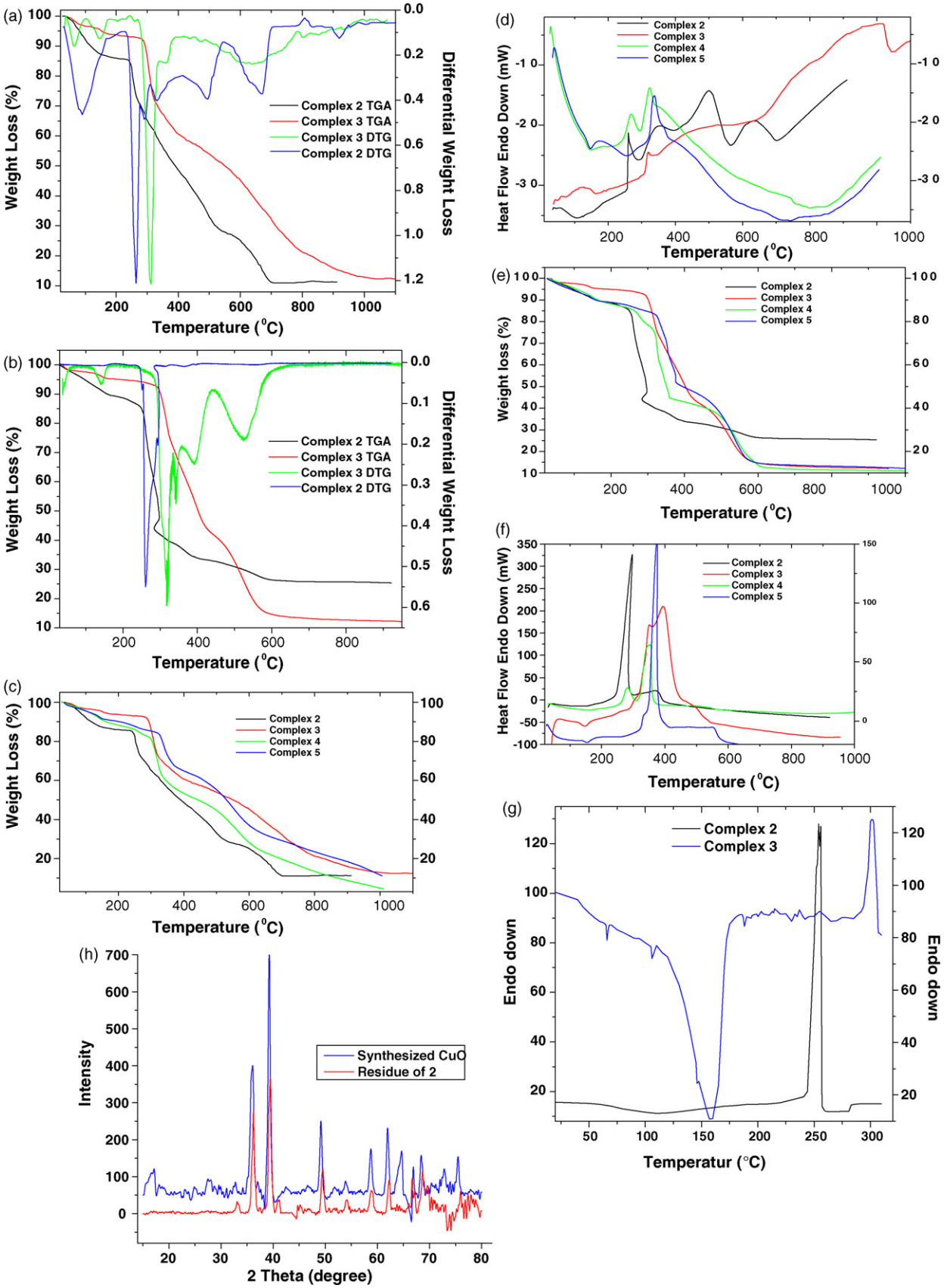

Fig. 4. (a) TGA and DTG thermograms of 2 and 3 under nitrogen atmosphere. (b) TGA and DTG thermograms of 2 and 3 under air atmosphere. (c) TGA curve of the complexes 2, 3, 4 and 5 under nitrogen atmosphere. (d) DTA curve of the complexes 2, 3, 4 and 5 under nitrogen atmosphere. (e) TGA curve of the complexes 2, 3, 4 and 5 under air atmosphere. (f) DTA curve of the complexes 2, 3, 4 and 5 under air atmosphere. (g) DSC curves of the complexes 2 and 3 and (h) PXRD pattern of residue of 2 and CuO.

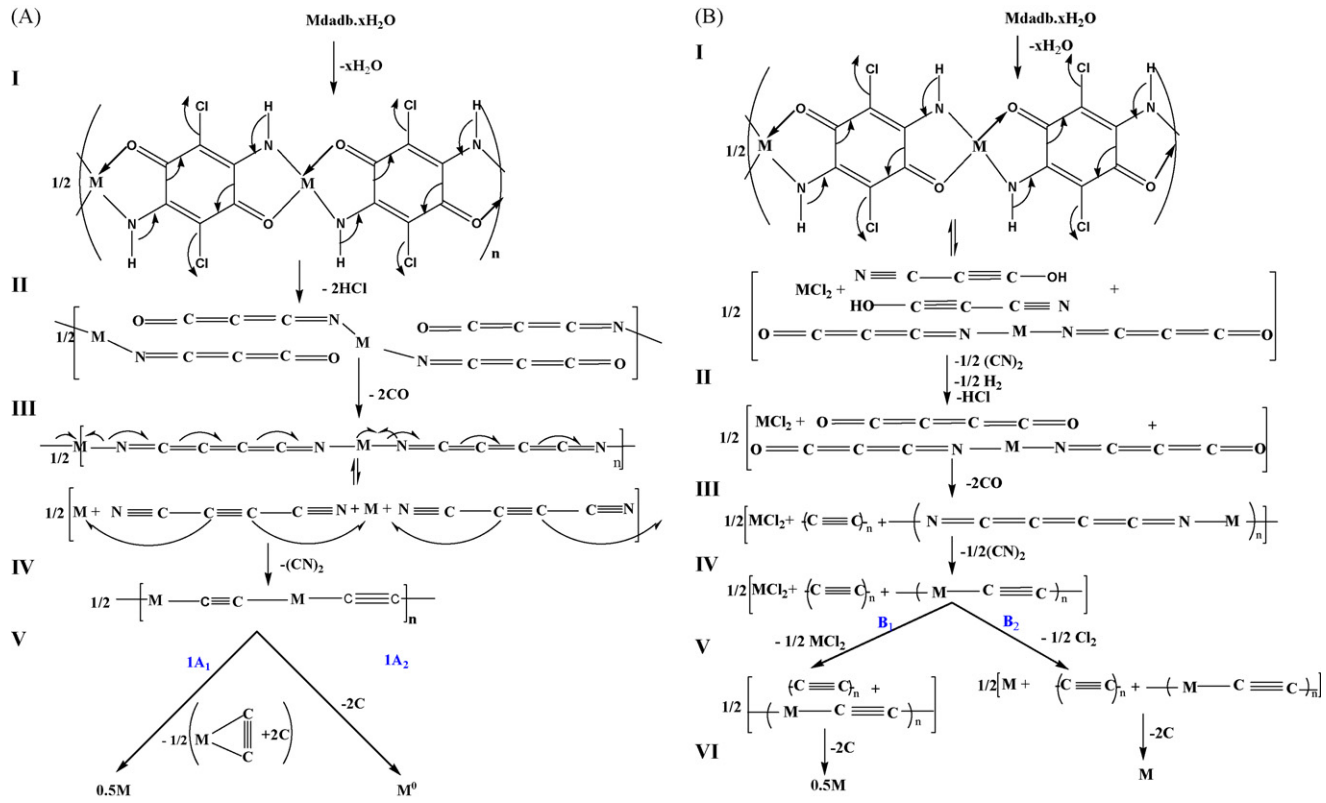

Scheme 1. Thermal degradation of metal complexes under nitrogen atmosphere.

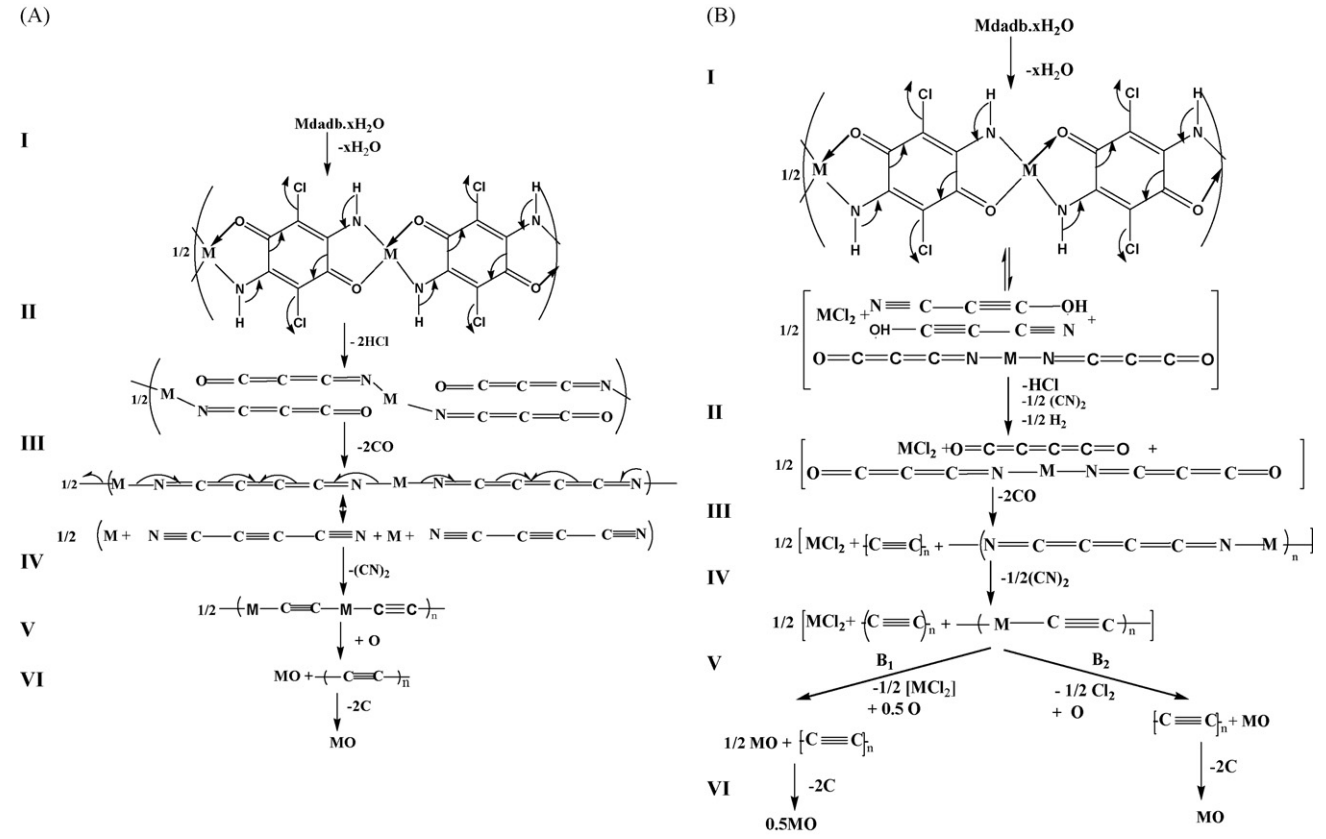

Scheme 2. Thermal degradation of metal complexes under air atmosphere.

curve matches with weight loss calculated for this complex following Scheme 1A indicating Scheme 1A being followed during thermal degradation of 2 under nitrogen atmosphere.

Experimentally observed weight loss corresponding to the loss of two CO molecules under 3rd step of decomposition matches with calculated value following Scheme 1A and that calculated under Scheme 1B falls on the curvature of DTG peak. Calculated weight loss under 4th step of the thermal degradation following Scheme 1B and A are calculated to be 8.29 and 16.58%, respectively. Weight loss obtained from TGA curve for this step matches with that calculated for Scheme 1A. At end of 4th step the residue obtained corresponds to the expected composition CuC_2 and rule out the possibility of thermal degradation under Scheme 1B. This may lose two mole of carbon (7.65%) and yield a metallic copper residue ~20.28% as shown in Scheme $1A_2$. However, TGA curve shows the weight loss of 18.4% leaving behind a residue of 9% which is very close to 1/2 mole of copper metal consistent with Scheme $1A_1$. This indicate that under 5th step of thermal degradation 1/2 mole of copper metal is evaporated/volatilized along with two mole of carbon probably by forming copper acetylide [28] (however it is expected to be unstable and explode at that temperature).

Thermal degradation of 2 under air is also expected to follow either of the two fragmentation pattern shown by Scheme 2A and B. The calculated weight losses corresponding to the Scheme 2A and B for 2 under air are given in S.I. Table 1(b) in parenthesis preceded by observed values from TGA curve. Apart from water loss under 1st step of thermal degradation, the losses under 2nd step in air is also taking place at almost same temperature as in the case of that under nitrogen atmosphere (Fig. 4b). The loss of CO molecules at third step of degradation under air starts at much lower temperature even before the completion of HCl loss. Temperature ranges for the losses of HCl and CO molecules under 2nd and 3rd steps, respectively, are so close to each other that they yield one broad peak in their DTG (S.I. Fig. 1b) and DTA curves (Fig. 4f). The experimental data of weight loss at end of third step of degradation does not match with that calculated by Scheme 2B, however, it matches with that calculated from Scheme 2A. Weight loss from the TGA curve indicates that thermal degradation under IVth step, i.e. loss of $(CN)_2$ molecule and Vth step, i.e. absorption of oxygen are taking place simultaneously. Weight loss under this combined step also matches with degradation Scheme 2A. The loss of two mole of carbon at last step of thermal degradation is also consistent with degradation Scheme 2A for the thermal degradation of 2 under air atmosphere. The residual mass corresponds with one mole of CuO. Powder XRD spectrum (Fig. 4h) of residue of 2 matches with X-ray diffractogram of freshly prepared CuO following literature procedure [29] and JCPDS file of CuO (5-661) confirms the formation of CuO as residue under air atmosphere.

Second stage of thermal degradation of 2 starts ~200 °C under air as well as nitrogen atmosphere. The loss of CO molecule at third stage of decomposition of 2 under the air starts at lower temperature (276 °C) than that under nitrogen atmosphere (315 °C). Thus it appears that rate of elimination of CO molecule is accelerated under air atmosphere, whereas elimination of HCl molecule take place at almost same temperature under both atmospheres. Fourth stage of decomposition under nitrogen atmosphere the weight loss corresponds to the loss of $(CN)_2$ molecule in the temperature range 425–550 °C, whereas under air atmosphere loss of $(CN)_2$ molecule take place at lower temperature (300–420 °C) accompanied by a gain of 1/2 mole of oxygen to form CuO. Fifth stage of decomposition under nitrogen atmosphere the weight loss corresponds to the loss of 1/2 mole of copper and one mole of C_2 molecule, whereas in the presence of air the weight loss is consistent with the loss of 2 mole of carbon. The DTA curve corresponding to the loss of 1/2 mole of copper and 2 mole of carbon under nitrogen atmosphere exhibits a broad exothermic peak at 633 °C. Loss of copper metal and 2 mole of carbon from 2 under nitrogen atmosphere is found to be exothermic, however, it is expected to be endothermic. This points toward some exothermic reaction taking place during with loss of copper metal and 2 mole of carbon. Further, the volatilization of copper metal is not possible in this temperature range, however, polymeric organometallic compound expected to be formed (Scheme 1a) may break into volatile copper acetylide. Presence of exothermic peak in DTA may arise due to explosion of copper acetylide after volatilization in vicinity of crucible at this temperature range. This heat is expected to aid in evaporation of 2 mole of carbon which is otherwise expected to be endothermic process under nitrogen atmosphere. Weight loss corresponding to the loss of 2 mole of carbon under air does not exhibit any indication of heat flow in its DTA curve. Finally, the residue obtained under nitrogen atmosphere at 700 °C corresponds to 1/2 mole of metallic copper, whereas that under air to one mole of CuO. The DTA curve under nitrogen exhibits endothermic peaks corresponding to water loss (109 °C), however, exothermic peaks are observed corresponding to the loss of HCl molecules (264 °C). Observed exothermic peaks during the loss of CO (351 °C), $(CN)_2$ (502 °C), and copper acetylide and 2 mole of carbon (633 °C) are unexpected because breaking of CO, —C≡N and C_2 molecules from ligand residue should be endothermic under nitrogen atmosphere. The DTA curve under air exhibits an endothermic peak corresponding to the loss of water and an strong exothermic peak combined together for the loss of HCl and CO molecules where temperature goes upto 297 °C. Next step of degradation is expected to be endothermic corresponding to loss of $(CN)_2$ molecules. Its DTA and TGA curves (Fig. 4e and f) show that loss of this step starts from ~285 °C indicating non-ideal nature of these curves. Thus, the temperature of the sample increased above the programmed temperature due to the exothermic effect in second and third step followed by a decrease of such temperature in endothermic forth step of degradation, producing an effect in the shape (backward curvature) of TGA and DTA curves. It appears that time-temperature profiles seem to be affected by the strong exothermic character of the previous processes. The DTA curve shows slightly but gradually increasing exothermic peak from 297–372 °C with peak maxima at 372 °C due to absorption of oxygen molecules (fifth step of degradation) accompanied with forth step. Thus it can be concluded that loss of $(CN)_2$ molecules starts ~285 °C and absorption of oxygen starts at relatively higher temperature with highest rate ~370 °C The amount of residue consistent with one mole of CuO indicates that absorbed oxygen converts copper ion into CuO. However, there is no indication of heat flow during the loss of C_2 molecule under air atmosphere.

The weight loss observed (30.2%) upto 2nd step of degradation of 3 (S.I. Table 1(c)) is found to be intermediate between those calculated following Scheme 1A (31.55%) and Scheme 1B (28.26%). The weight loss observed (39.40%) from TGA curve upto 3rd step of weight loss (loss of one CO molecule) also falls at intermediate position between those of Scheme 1A (41.26%) and B (37.97%). Therefore, based on above data no conclusion can be drawn. Weight loss upto forth step of degradation calculated by Scheme $1A_2$ (69%) falls on the curvature of DTG peak ~710 °C and weight loss calculated by Scheme $1A_1$ (84.5%) also falls on the curvature of the DTG curve, therefore, it may be concluded that none of the Scheme $1A_1$ or $1A_2$ is applicable for the thermal degradation of 3 under nitrogen atmosphere. However, experimentally observed weight loss (80.8%) upto 4th step of degradation matches with calculated weight loss on the basis of Scheme $1B_1$ (80.34%). It is worth to be mentioned that boiling point of $ZnCl_2$ is 732 °C [30], therefore, it may volatilize in the temperature range (400–825 °C) during 4th step of thermal losses. Observed weight loss (7.7%) from TGA curve under fifth step fits well with weight loss calculated from Scheme 1B (8.32%). Thus, weight loss upto 4th step, weight loss dur-

ing 5th step and overall residue obtained after thermal degradation under nitrogen atmosphere match with the weight loss calculated on the basis of Scheme 1B_1. It may be concluded that 3 follows the degradation patterns shown by Scheme 1B under nitrogen atmosphere.

Theoretically calculated weight loss (31.55%) upto 2nd step of degradation (S.I. Table 1(d) and Fig. 4b) following Scheme 2A falls on the curvature of DTG peak corresponding to the loss of CO molecules, therefore, the pattern of Scheme 2A being followed for the degradation of 3 under air is unlikely. The experimentally observed weight loss (28%) upto 2nd step of thermal degradation is consistent with calculated value following Scheme 2B (28.26%). Calculated weight loss upto third step of thermal degradation (for the loss of one CO molecule) following Scheme 2A (41.26%) is inconsistent with experimentally observed weight loss (37.3%) falling on the curvature of the DTG curve for the next step of degradation. However, weight loss obtained from TGA and DTG curves (Fig. 4b) upto 3rd step of degradation matches with calculated weight loss by Scheme 2B (37.97%). These results indicate that unlike complex 2 the complex 3 does not follow the degradation pattern shown by Scheme 2A rather it follows the Scheme 2B. Calculated weight loss at end of 4th step of degradation following Scheme 2A falls on curvature of the DTG curve for the subsequent step of thermal degradation. However, weight loss calculated following Scheme 2B matches with weight loss obtained from TGA curve corroborated by the DTG curve. Weight loss upto end of 5th and 6th steps of degradation are calculated to be 71.78% by both Scheme 2A and B_2 which is inconsistent with weight loss observed from TGA curve (86.1%) for 3 under air. However, weight loss calculated by Scheme 2B_1 (85.89%) matches with experimentally observed from TGA curve. Complex 3 leaves a residue corresponding to 1/2 mole of ZnO (13.9%, theoretical 14.11%) consistent with expected residue from the Scheme 2B_1. Thus, it may be concluded that 3 under air follows the thermal degradation pattern presented under Scheme 2B. Finally, it may be summarized that 3 leaves a residue corresponding to 1/2 mole of metallic zinc under nitrogen and 1/2 mole of ZnO under air atmosphere on thermal degradation, whereas 2 provides a residue corresponding to 1/2 mole of metallic copper under nitrogen and one mole of CuO under air atmosphere.

Weight loss in second stage of thermal degradation of 3 under both atmosphere (nitrogen and air) are completed almost at the same temperature ~335 °C and corresponds to the loss of one mole HCl molecule and 1/2 mole of $(CN)_2$ and hydrogen molecules (Schemes 1B and 2B). The loss of HCl molecules begins at relatively higher temperature (300 °C) in 3 as compare to that in 2 (~255 °C) under both environments. Weight loss corresponds to the loss of one CO molecule at third stage of decomposition of complex 3 under nitrogen as well as air atmospheres, however, two moles of the CO molecules are lost under third step of decomposition of complex 2. The corresponding DTG peak is obtained at 380 and 338 °C under nitrogen and air atmosphere, respectively, for 3. From these results it can be concluded that air accelerates the loss of CO molecules. Further, third step of decomposition takes place at higher temperatures for the complex 3 under both atmospheres than those of corresponding decomposition for the complex 2.

Weight loss under fourth step of decomposition of complex 3 corresponds to the loss of half mole of $(CN)_2$ and one mole of CO molecules under air, whereas under nitrogen atmosphere evaporation of $ZnCl_2$ is also associated along with above (weight loss at V step in Scheme 2B). This step of decomposition is completed at lower temperature under air than that of under nitrogen atmosphere. The losses of CO and $(CN)_2$ molecules from 2 under nitrogen atmosphere exhibit exothermic peaks in its DTA curve but in case of 3 there is no indication of exothermic peaks, however an endothermic peak observed in the DTA curve at 633 °C corresponds to forth step of thermal degradation under nitrogen atmosphere. Forth step of decomposition of complex 3 under air exhibits an exothermic DTA peak at 394 °C whereas complex 2 exhibits at 372 °C. This indicates that this step of thermal degradation undergoes at lower temperature in presence of copper ions as compared to that of zinc ion. It is worth to be mentioned that absorption of oxygen also take place in complex 2 under forth step of degradation whereas oxygen absorption takes place under fifth step of degradation of complex 3. The $ZnCl_2$ and two mole of carbon are lost under fifth stage of decomposition accompanied with absorption of 1/4 moles of oxygen to form half mole of ZnO. The residual mass after thermal degradation of 3 under air corresponds to 1/2 mole of ZnO, whereas that in case of complex 2 it corresponds to one mole of CuO. Fifth stage of decomposition under air takes place at much lower temperature for the complex 3 as compare to that under nitrogen atmosphere. At fifth step of thermal degradation of 3 under nitrogen atmosphere, weight loss corresponds to the loss of two mole of carbon in the temperature range 825–1100 °C accompanied with endothermic peak at ~1043 °C. Thus two mole of carbon are lost at higher temperature from 3 as compare to that from 2 under nitrogen atmosphere. The residual mass corresponds to 1/2 moles of metals from both the complexes 2 and 3 under nitrogen atmosphere.

Thermogravimetric data (S.I. Table 1(c–d)) of the complexes 4 and 5 indicate that water is lost at first stage of degradation like 2 and 3. The thermal degradation in subsequent steps for the heterobimetallic complexes have been interpreted assuming that degradation of ligand moiety around copper and zinc metal ions follow the degradation pattern of 2 and 3, respectively. Thus, in case of complex 4, it is assumed that one mole of HCl liberated molecule react with all the zinc ions present and converts it into $ZnCl_2$ and ligand moiety around copper ion follows the degradation pattern of scheme A as in case of complex 2. In case of complex 5, experimental weight loss data matches with calculated data assuming that half of zinc ions react with HCl, i.e. if follows the pattern of scheme B as in complex 3 and copper ions do not react with HCl and ligand moiety around copper follows the pattern of scheme A as in complex 2. Obviously, all the complexes absorb oxygen and form metal oxides as residue under air atmosphere.

Second step of thermal degradation of heterobimetallic complexes (4 and 5) under both atmosphere (nitrogen and air) corresponds to the losses of half mole of each of $(CN)_2$ and H_2 molecules whereas in cases of complex 2 two moles of HCl molecules and in case of complex 3 this step is consistent with loss of one mole of HCl and half mole of each of $(CN)_2$ and H_2 molecules. From TGA and DTG thermograms of 4 and 5 it is obvious that 2nd step of degradation starts at lower temperature than those for the 2 and 3 under both atmospheres. Thus it appears that bimetallic complexes are different from those of monometallic complexes 2 and 3. In case of 3, there is no DTG/DTA peak in the temperature range 200–300 °C indicating major losses under 2nd step of decomposition to take place at higher temperature (>300 °C). The DTA peak for 2 and 4 in the temperature range 200–300 °C under both atmosphere (nitrogen and air) are exothermic, whereas for the complex 5 it is endothermic. In case of the complex 4 one HCl molecules are eliminated from the ligand moiety around copper metal ions which are expected to react with zinc metal ions to form 1/2 moles of $ZnCl_2$ and hydrogen molecules, both of these steps are expected to be exothermic. Residual part of ligand moiety which becomes free from metal under same step of thermal degradation loses 1/2 moles of $(CN)_2$ molecules and is also expected to be endothermic step. Therefore, the heat flow is expected to be resultant of all the processes under this step and is observed as weakly exothermic DTA peak for the complex 4 in the both envi-

ronment. In case of complex 5 the amount of weight loss observed from TGA and DTG thermograms under second step of thermal degradation is consistent with elimination of 1/2 mole of $(CN)_2$ and hydrogen molecules. Further the loss under 2nd step is taking place with very slow speed in case of heterobimetallic complexes, whereas in case of 3rd step the loss is taking place with relatively faster speed as is evident from TGA and DTG curves (Fig. 4c and e). There are strong peaks in DTG curves of the complexes 2 (∼263 °C) and 3 (∼314 °C) corresponding to 2nd step of thermal degradation under both atmosphere. Presence of weak peaks at 262 and 253 °C under nitrogen and 273 and 262 °C under air atmospheres in the DTG curves of complexes 4 and 5 (S.I. Fig. 1a and b), respectively, supports the above interpretations. Presence of weak endothermic peak in the DTA thermograms of complex 5 at 255 and 267 °C under nitrogen and air atmospheres, respectively (Fig. 4d and f) unlike other complexes are consistent with DTG thermogram. Thus, as the amount of copper is lowered in heterobimetallic complexes the amount of heat evolved during the thermal degradation is reduced in the temperature range 200–300 °C and finally it becomes weakly endothermic as in case of 5. In third stage of degradation involves the loss of one mole of each HCl and CO molecules from complex 4 and one mole of HCl and 1/2 mole of CO molecules from complex 5 under nitrogen atmosphere. Under air atmosphere the weight loss is consistent with the loss of one mole of HCl and 1/2 mole of CO molecules from former complex whereas only one mole of HCl from the latter complex. However in case of 2 and 3 this step involves the loss of two and one moles of CO molecules, respectively under both atmospheres. DTA curves show that this step is exothermic in thermal degradation of 2 as well as heterobimetallic complexes 4 and 5 under both atmospheres because there is loss of HCl along with CO molecules. The weight loss at forth step of degradation of complexes 4 and 5 under nitrogen atmosphere matches with calculated losses of remaining CO, $(CN)_2$, and half of copper metal is being lost as CuC_2 and appropriate amount of zinc metal as $ZnCl_2$ assuming the part of complex containing copper ions undergoes degradation in same way as complex 2 and remaining part containing zinc ions as complex 3. Under air atmosphere weight loss at forth step of degradation corresponds to the loss of remaining CO and half mole of $(CN)_2$ molecules of complex 4, whereas in case of the complex 5 the weight loss corresponds to the loss of two CO molecules. Under fifth step of degradation the weight loss from complex 4 match with loss of 1/4 mole of $ZnCl_2$ and remaining 1.5 mole carbon under nitrogen and loss of 1/2 mole of $ZnCl_2$ and $(CN)_2$ molecules, two mole carbon and absorption of 1/4 mole of oxygen under air atmosphere. The residue obtained after thermal degradation of complex 4 corresponds to 1/4 mole of metallic copper under nitrogen atmosphere and 1/2 mole of CuO under air. Similarly weight losses under fifth step of thermal degradation match with losses of 3/8 mole of $ZnCl_2$, and remaining amount of carbon under nitrogen and losses of 1/2 mole of $(CN)_2$ and $ZnCl_2$ molecules and two mole of carbon and absorption of 1/4 mole of O_2 molecule under air atmosphere. The residue obtained at end of thermal degradation corresponds to the mixture of metallic copper and zinc under nitrogen and mixture of oxides of copper and zinc under air atmosphere.

4. Conclusion

First stage of weight loss corresponds to the loss of water molecule under air as well as nitrogen atmosphere for all the complexes. DSC thermogram of complex 2 dried over calcium chloride under vacuo for a period of 20 days exhibits no peak in the temperature range 40–240 °C indicating the presence of non-coordinated nature of water molecules, i.e. crystalline water. Presence of exothermic peaks in the DTA curve of some of the complexes in the temperature range RT–60 °C indicate absorption of moisture by the samples on exposure to air. The amounts of water molecules absorbed depend upon the relative humidity present in the air.

Second step of thermal degradation (loss of HCl or $(CN)_2$ molecules and hydrogen) take place at almost same temperature under both (nitrogen and air) atmosphere. However, the second step of degradation take place at lower temperature in complex 2 than that of complex 3, i.e. by changing the metal ion from zinc to copper the thermal degradation process is accelerated. It may be concluded that copper (II) metal ion having unpaired electron catalyzed the removal of HCl molecules. Third step of thermal degradation (loss of CO molecules) are completed at lower temperature in air than that under nitrogen atmosphere for all the complexes. Thus it appears that oxygen helps in removal of CO molecules under air. Under air atmosphere CO is expected to be converted into CO_2 and liberates heat. It is this heat which accelerates the rate of removal of other fragments at lower temperature under air as compared to that under nitrogen atmosphere from all the complexes 2, 3, 4 and 5. Fourth step of decomposition involves loss of $(CN)_2$ molecules under nitrogen and absorption of oxygen in addition to the loss of $(CN)_2$ under air from complex 2, whereas in case of complex 3, in addition to above losses the left over CO elimination take place in air and under nitrogen atmosphere evaporation of zinc chloride also take place this step. Thermal degradation is completed at lower temperature under air than that under nitrogen like third step for all the complexes studied by thermo-gravimetrically. Forth step of degradation is completed at lower temperature in case of copper complex 2 than that of zinc complex 3 which is more distinct under nitrogen atmosphere. Fifth step of decomposition involves the loss of half mole of metallic copper and two mole of carbon under nitrogen atmosphere whereas in case of air atmosphere only two mole of carbon is lost from complex 2. In case of zinc complex 3, the loss of two mole of carbon takes place under nitrogen whereas under air atmosphere the loss of two mole of carbon is accompanied with loss of $ZnCl_2$ and absorption of oxygen. Fifth step is endothermic under nitrogen, whereas, it is weakly exothermic under air atmosphere. Presence of exothermic peak in DTA curve under air atmosphere presumably arises due to reaction of carbon atoms with oxygen under air to form CO and CO_2 in the temperature range 450–600 °C and liberating heat. Due to this liberated heat the thermal degradation (mainly the loss of C_2) under fifth step is also completed at much lower temperature under air. However, there is no indication of exothermic peak in case of complex 4 and 5. The loss of zinc chloride, a fraction of $(CN)_2$ molecules are associated under this step in the complex 4 and 5 and they are expected to be endothermic, therefore, overall effect is weakly endothermic. In case of complex 2 the residue corresponds to half mole of copper metal under nitrogen atmosphere, whereas same sample under air yields a residue corresponding to one mole of CuO. These result indicate that half mole of copper is lost/evaporated under nitrogen atmosphere probably by forming a complex with C_2 molecules (acetylide moiety). Sublimation/evaporation of metallic copper is unlikely around this temperature range, however, polymeric organometallic compound expected to be formed during thermal degradation of the complex may break into volatile copper acetylide. Presence of exothermic peak at 633 °C in DTA curve is expected to arise due to explosion of copper acetylide just after volatilization in vicinity of crucible at this temperature range. This heat may aid in evaporation of carbonacious residue, otherwise, it should be endothermic process under nitrogen atmosphere and loss of it should be completed at much higher temperature as in the case of complex 3. In case of complex 3 the residue obtained from TGA curve corresponds to the half mole of metallic zinc and zinc oxide under nitrogen and air atmosphere, respectively. These observations are consistent with degradation pattern proposed under scheme A and B for

the complex 2 and 3, respectively. The residue obtained from thermal degradation of the heterobimetallic complex 4 corresponds to 1/4 mole of metallic copper (5.3%) and 1/2 mole of copper oxide (12.62%) under nitrogen and air atmospheres, respectively. These results indicate that ligand moiety (dadb) around copper and zinc metal ions undergo degradation according to scheme A and B, respectively, in heterobimetallic complex 4. Further, since the copper and zinc metal ions are expected to be in alternate position in the polymeric chain, therefore, HCl molecules liberated by the heterobimetallic complexes from copper sites completely react with zinc metal ions and form $ZnCl_2$ and subsequent fragmentation follows. Thus, all the zinc metal ions are expected to form zinc chloride which is evaporated/volatilized whose boiling point [30] is 732 °Cs and the residue corresponds to copper metal/copper oxide depending upon the environment under which degradation is taking place. For the equimolar mixture of 2 and 3, the final residue is expected to be ~10.55% consistent with composition 1/4 mole of copper and 1/4 mole of zinc metal ion following respective degradation pattern of complexes 2 and 3, respectively, under nitrogen atmosphere. Similarly under air atmosphere the residue is expected to be consistent with composition 1/2 mole of copper oxide and 1/4 mole of zinc oxide following respective degradation pattern of the complexes 2 and 3. These thermal degradation results do not match with residue obtained from the complex 4 further confirms the distinct identity of heterobimetallic complex 4 rather than equimolar mixture of 2 and 3. Similarly, residue obtained from degradation of complex 5 also can be explained. A careful observation of TGA and DTA curves indicate that each of the complexes follows its characteristics thermal degradation curves depending upon amount of respective metal ion contribution into it.

Acknowledgements

Authors are thankful to Head, Department of Chemistry for providing laboratory facilities, magnetic moment measurements, recording of IR, UV–visible spectra and DSC thermograms. Financial assistant from UGC New Delhi in form of a project is gratefully acknowledged. Thanks are also due to SAIF, Madras and Cochin for providing TGA, DTG and DTA thermograms. Last but not least the authors are thankful to the reviewers for their useful comments and clarifying our understanding on our observed non-ideal TGA and DTA curves.

Appendix A. Supplementary data

Supplementary data associated with this article can be found, in the online version, at doi:10.1016/j.tca.2010.07.019.

References

[1] R.L. Prasad, A. Kushwaha, Suchita, M. Kumar, R.A. Yadav, Spectrochim. Acta A 69 (2008) 304–311, and references therein.
[2] S. Kulpe, Acta Crystallogr. Sect. B-Struct. Sci. 25 (1969) 1411–1416.
[3] S. Kulpe, D. Leupold, S. Daehne, Angew. Chem. Int. Ed. 5 (1966) 599–600.
[4] R.L. Prasad, A. Kushwaha, R.J. Butcher (communicated).
[5] S. Kawata, S. Kitagawa, I. Furuchi, C. Kudo, H. Kamesaki, M. Kondo, M. Katada, M. Munakata, Mol. Cryst. Liq. Cryst. 274 (1995) 179–185.
[6] C. Creutz, H. Taube, J. Am. Chem. Soc. 95 (1973) 1086–1094.
[7] M.D. Ward, Chem. Soc. Rev. 24 (1995) 121–134.
[8] T. Yamamoto, T. Maruyama, Z-h. Zhou, T. Ito, T. Fukuda, Y. Yoneda, F. Begum, T. Ikeda, S. Sasaki, H. Takezoe, A. Fukuda, K. Kubota, J. Am. Chem. Soc. 116 (1994) 4832–4845.
[9] G.G. Condorelli, G. Malandrino, I. Fragala, Chem. Mater. 7 (1995) 2096–2103.
[10] P. Poizot, S. Laruelle, S. Grugeon, L. Dupont, J.M. Taracon, Nature 407 (2000) 496–499.
[11] A.H. Mac Donald, Nature 414 (2001) 409–410.
[12] R.V. Kumar, Y. Diamant, A. Gedanken, Chem. Mater. 12 (2000) 2301–2305.
[13] X.P. Gao, J.L. Bao, G.L. Pan, H.Y. Zhu, P.X. Huang, F. Wu, D.Y. Song, J. Phys. Chem. B 108 (2004) 5547–5551.
[14] T. Maruyama, Sol. Energy Mater. Sol. Cells 56 (1998) 85–92.
[15] J. Ramirez-Ortiz, T. Ogura, J. Medina-Valtierra, S.E. Acosta-Ortiz, P. Bosch, J.A. De Los Reyes, V.H. Lara, Appl. Surf. Sci. 174 (2001) 177–184.
[16] Y.W. Cao, R. Jin, C.A. Mirkin, J. Am. Chem. Soc. 123 (2001) 7961–7962.
[17] M. Cao, C. Hu, Y. Wang, Y. Guo, C. Guoa, E. Wanga, Chem. Commun. (2003) 1884–1885.
[18] T. Allmendinger, Macromol. Chem. Phys. 198 (1997) 4019–4034.
[19] B.S. Furmiss, A.J. Hannaford, B. Rogers, P.W.G. Smith, A.R. Tatchell, Vogel's Text Book of Practical Organic Chemistry, 4th ed., ELBS, 1978.
[20] L.F. Fieser, E.L. Martin, J. Am. Chem. Soc. 57 (1935) 1844–1849.
[21] J.V. Folgado, R. Ibanez, E. Coronado, D. Beltran, J.M. Savariault, J. Galy, Inorg. Chem. 27 (1988) 19–26.
[22] K. Nakamoto, Infrared and Raman Spectra of Inorganic and Coordination Compounds, 5th ed., Wiley Interscience, New York, 1997.
[23] L.V. Azaroff, M.J. Buerger, The Powder Method in X-ray Crystallography, McGraw-Hill, New York, 1958, p. 119.
[24] S.A. sallam, Trans. Met. Chem. 31 (2006) 46–55.
[25] B.N. Figgis, J. Lewis, Prog. Inorg. Chem. 6 (1964) 37–239.
[26] F.A. Cotton, G. Wilkinson, C.A. Murillo, M. Bochmann, Advanced Inorganic Chemistry, 6th ed., John Wiley & Sons, Inc., New York, 1999, p. 714.
[27] A.B.P. Lever, Inorganic Electronic Spectroscopy, Elsevier, Amsterdam, 1986, p. 376.
[28] A.M. Sladkov, L.Y. Ukhin, Russ. Chem. Rev. 37 (1968) 748–763.
[29] Z. Yang, J. Xu, W. Zhang, A. Liu, S. Tang, J. Solid State Chem. 180 (2007) 1390–1396.
[30] J.A. Dean (Ed.), Langes's Handbook of Chemistry, 13th International ed., McGraw-Hill Book Company, New Delhi, 1987.